



Full Length Research Manuscript

Optimization of Pulsed Laser Deposition Parameters for Single-Crystalline (011) Oriented Tetragonal Pzt Thin Films

Mahamudu Mtebwa

Department of Mechanical and Industrial Engineering, University of Dar es Salaam, Tanzania
Correspondence e-mail: mtebwa@udsm.ac.tz; ORCID: <https://orcid.org/0000-0003-1027-1296>

ABSTRACT

Recent advances in nanotechnology applications require the processing of high-quality thin films. A systematic study of the optimization of Pulsed deposition parameters for (110) oriented tetragonal PZT thin films is reported in this work. Prior to film deposition, a highly tetragonal $\text{Pb}(\text{Zr}_{0.5}, \text{Ti}_{0.95})$ or PZT 05/95 was selected to be deposited on (110) oriented Strontium titanate, SrTiO_3 substrate, STO(110) to insure small compressive misfit strain. Unlike SRO, the LSOM bottom electrode was then successfully grown at 620 °C, 1.0 J/cm² and a target-substrate distance of 3.9 cm. Finally, deposition parameters of PZT were progressively optimized through monitoring film morphological changes. Monocrystalline PZT films of different thicknesses with layer-by-layer growth mode were finally realized at a deposition temperature of 550 °C, laser energy of 1.0 J/cm², background pressure of 200 mTorr O₂, while deposition rate was 3 Hz and target-substrate distance of 3.1 cm. The optimal film growth rate was finally estimated to be 0.3 nm/100 Pulses.

ARTICLE INFO

Submitted: October 12, 2022

Revised: November 15, 2022

Accepted: December 8, 2022

Published: December 30, 2022

Keywords: PZT, SRO, LSOM, Thin Pulsed Laser Deposition, Epitaxy, film

INTRODUCTION

Lead Zirconate Titanate (PZT) is the most widely used material in electromechanical applications such as in actuators, transducers and energy harvesting due to its superior piezoelectric properties (Damjanovic, 1998). Chemically, PZT is a solid solution of lead titanate, PbTiO_3 (PTO) and lead zirconate and PbZrO_3 (PZO). PZT is also known for its superior ferroelectric and ferroelastic properties. Recent advances in thin film growth techniques have driven the modern study of complex ferroelectric oxide materials leading to the discovery of new multiferroic systems and the production of materials with non-equilibrium phases through domain engineering (Kim *et al.*, 2020; Mtebwa *et al.*, 2014). Domain engineering is the technique employed to

obtain the enhanced ferroelectric-related properties for conventional ferroelectric materials both in bulk ceramics (Wada *et al.*, 2007; Wada *et al.*, 2004; Wada and Tsurumi, 2004; Wada *et al.*, 1999), and most recently in thin films (Kim *et al.*, 2020; Baek *et al.*, 2017).. Single domain state can be archived by applying an electric field along the polar crystallographic orientation, in this case along [001] for tetragonal symmetry. However, it has been demonstrated that a high density of periodic domain patterns can be obtained by applying an electric field along one non-polar orientation of the single crystal sample in domain engineering (Wada *et al.*, 1998). This interesting observation opens up a wide range of possibilities for processing ferroelectric material, PZT in particular with desired domain patterns that suit a particular application.

In addition to film orientation, the nature of domain structures to be realized also depend upon the in-plane strain imposed by the substrate (strain engineering), as well as the processing conditions quality of thin films (Sun *et al.*, 2021; Schwarzkopf *et al.*, 2017; Vafaei *et al.*, 2013; Chu *et al.*, 2006). [011] is one of the special non-polar crystallographic directions for domain engineering which is of interest in this work. A number of studies have reported the processing of (110) oriented PZT thick films for electromechanical applications using different techniques including sol-gel (spin coating) (Ambika *et al.*, 2012; Ambika *et al.*, 2010) and pulsed laser deposition (PLD) (Vu *et al.*, 2015). However, these films are normally polycrystalline and sometimes textured due to misfit dislocations resulting from film strain relaxation as thickness increases. As for the thin films, a number of studies have already reported PZT films grown by PLD, however to our knowledge no studies have been reported on the effect

of deposition parameters. In this work, we report the systematic study on the optimization of PLD deposition parameters for (110) oriented tetragonal PZT thin films.

MATERIALS AND METHODS

PZT and Substrate Materials

In this work, a highly tetragonal Pb(Zr_{0.5}, Ti_{0.95}) or PZT 05/95 was selected to be deposited on (110) oriented Strontium titanate, SrTiO₃ substrate (STO(110)). The selection of film-substrate combination is determined by the nature of in-plane lattice mismatch, which can be estimated using $u = a_s - a_f/a_f$, where a_s and a_f are the in-plane lattice parameters of the substrate and the film respectively (Tagantsev *et al.*, 2010). As Table 1 shows, the PZT is expected to have a mismatch of about -0.28 % and -3.21 % along [100] and [1 $\bar{1}$ 0] directions of STO substrate respectively.

Table 1: PLD deposition parameters for LSMO and PZT 05/95 thin films.

Material	Lattice parameters (nm)		In-plane lattice parameters (nm)	
	a	c	[100]	[1 $\bar{1}$ 0]
PZ	0.3916	0.4142	0.3916	0.5700
STO(110)	0.3905	0.3905	0.3905	0.5522
Lattice Mismatch (%)			-0.28	-3.12

Substrate Treatment

STO(110) substrates consist of the stacking of alternating SrTiO⁴⁺ and O₂⁴⁻ layers (Biswas *et al.*, 2011). Since substrate termination is among the factors that determine thin film growth mode (Koster *et al.*, 2012; Bachelet *et al.*, 2009); STO(110) substrate treatment to attain TiO⁴⁺ rich topmost surface was conducted using the well-established procedures (Biswas *et al.*, 2011). The treatment procedure consists of the following steps:

- (i) Cleaning the substrates with acetone and alcohol (e.g Isopropanol or methanol) and performing ultrasonic soaking in deionized (DI) for about 30 minutes to dissolve a

water-soluble SrO into strontium hydroxide.

- (ii) Etching with buffered HF solution with a pH of about 4.5 for up to 15 seconds to selectively etch away strontium hydroxide

- (iii) Cleaning again the substrates with alcohol and,

- (iv) anneal the substrates at about 1000 °C for 1-3 hours to get an atomically flat surface with step terraces whose height is equal to single unit cell size.

Pulsed laser Deposition Method

In this work, both the bottom electrodes and PZT thin film were deposited by using the pulsed deposition technique (PLD). In this physical vapour deposition technique, materials from a target with desired chemical composition are evaporated and deposited on the substrate using high-power laser pulses (Antoni and Stock, 2021; Chrisey and Hubler, 2003; Willmott and Huber, 2000). As shown in Figure 1, the basic components of a PLD are a vacuum chamber, a rotating target holder also known as a carousel, a laser generator and oxygen pressure.

a set of optics for focussing the laser beam. For different substrate–film materials combinations, the film quality depends upon PLD parameters namely: Laser energy or Fluence (Jcm^{-2}), Deposition temperature ($^{\circ}C$), Vacuum pressure (mTorr), Deposition frequency (Hz) and Substrate-Target distance (cm). The combination of all these parameters in turn determines the film deposition or growth rate which is measured in nm/100 Pulses. For perovskite materials such as those used in this work, the vacuum pressure is controlled by background.

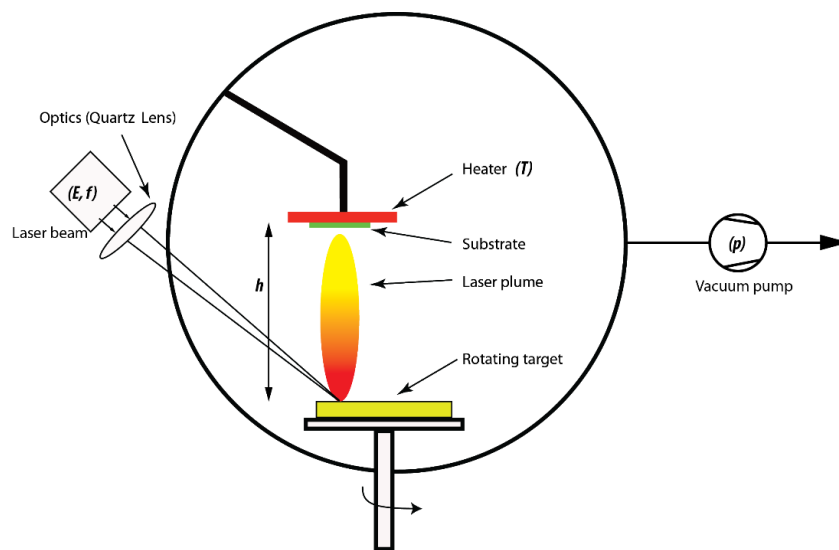


Figure 1: Schematic diagram of a Pulsed Deposition Setup modified from Mtebwa and Setter (2022). The deposition temperature (T) and vacuum pressure (p) are controlled by an electric heater and vacuum pump respectively; whereas, both the laser energy and deposition frequency are controlled by the laser generator.

RESULTS AND DISCUSSION

Substrate Treatment

Figure 2 (a) below shows the AFM image of the surface morphology of the treated STO (110) substrate. Figure 2 (b) indicates the plotted cross-sectional profile of the substrate, showing the atomic step height. The distance between the steps is approximately equal to 0.276 nm consistent with results reported in the literature (Biswas *et al.*, 2011).

Surface Topology Characterization of SRO and LSMO Bottom Electrodes

When depositing the bottom electrode, the first attempt was to grow SRO on BFH-treated STO(110) substrate. Although the right SRO phase was crystallized, it was not possible to achieve step flow growth mode. As shown in Figure 3, AFM topography showed selective film nucleation and poor surface diffusion suggesting that single surface termination of the STO(110) substrate was not achieved by chemical treatment.

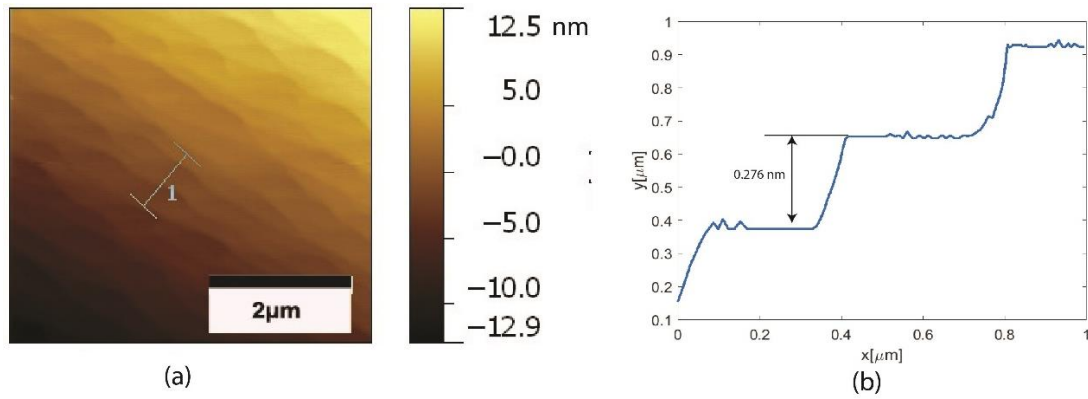


Figure 2: Treated STO(110) substrate: (a) AFM topography of ST(110) substrate. (b) Surface profile showing atomic steps.

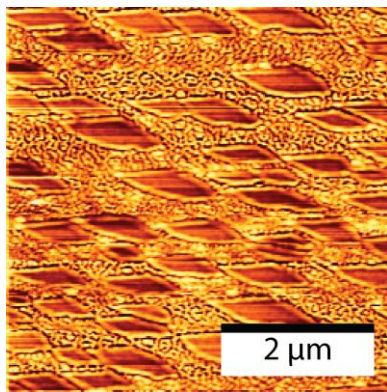


Figure 3: AFM topography of SRO thin film on STO(110) substrate showing selective nucleation due to multiple terminations of the substrate surface.

After unsuccessful results with SRO, the next attempt involved the use of LSMO as a bottom electrode. This follows similar attempts that have been reported whereby LSMO thin films were grown on untreated STO(110) for investigation of LSOM magnetic properties

(Majumdar *et al.*, 2013; Boschker *et al.*, 2010; Ma *et al.*, 2009)..

Figure 4 shows the progress in LSMO film quality improvement as the PLD deposition parameters were optimized. The grainy texture film topology in Figure 4 (a) was modified to preferentially elongated grainy features shown in Figure 4 (b) by decreasing the growth rate; by increasing the substrate-target distance from 2.7 cm to 3.9 cm. The hole-like structures (in Figure 4 (b)) in between the elongated structures suggested a high surface diffusion rate. Therefore, the surface diffusion rate was reduced by decreasing the growth temperature from 750 °C down to 620 °C, which resulted in the desirable step flow growth mode shown in Figure 4 (c). Finally, the small particles observed in Figure 4 (c) were eliminated by decreasing laser energy density from 1.5 to 1.0 J/cm².

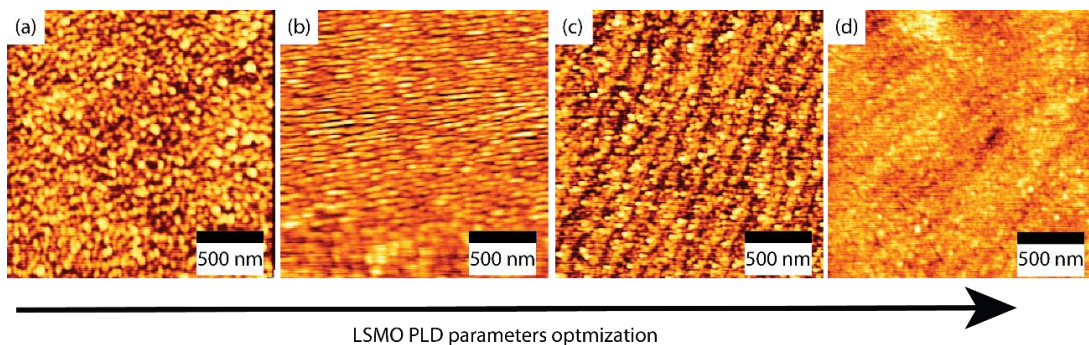


Figure 4: AFM topography of LSMO thin film on STO(110) substrate showing film growth improvements during optimization of PLD parameters.

Surface Topology Characterization of PZT Thin films

PZT 05/95 thin film quality growth mode was also improved through varying PLD parameters as shown in Figure 5. Grainy particles-like features also known as islands, which are associated with high growth rates were eliminated through an increase in substrate-target distance from 2 cm to 3.1cm (Figure 5 (a)-(c)). Poor atomic/molecular surface diffusion which normally results in hole-like features in between the elongated structures improved through decreasing growth temperature from 575 °C to 550 °C

(Figure 5 (c)-(e)). Figure 5 (e) shows a mix of short-range layer-by-layer growth mode underneath or mixed with island growth, suggesting that the high growth mode is still dominating. Therefore, the film growth rate was further reduced by decreasing laser energy down to 1.0 J/cm²; which in turn transformed the island growth mode in Figure 5 (e) to step flow growth mode in figure Figure 5 (f). Optimized PLD conditions for both LSMO and PZT 05/95 thin films are shown in Table 2. The roughness of the films at optimized conditions for both LSMO and PZT thin films is in the range of about 0.15-0.2 nm.

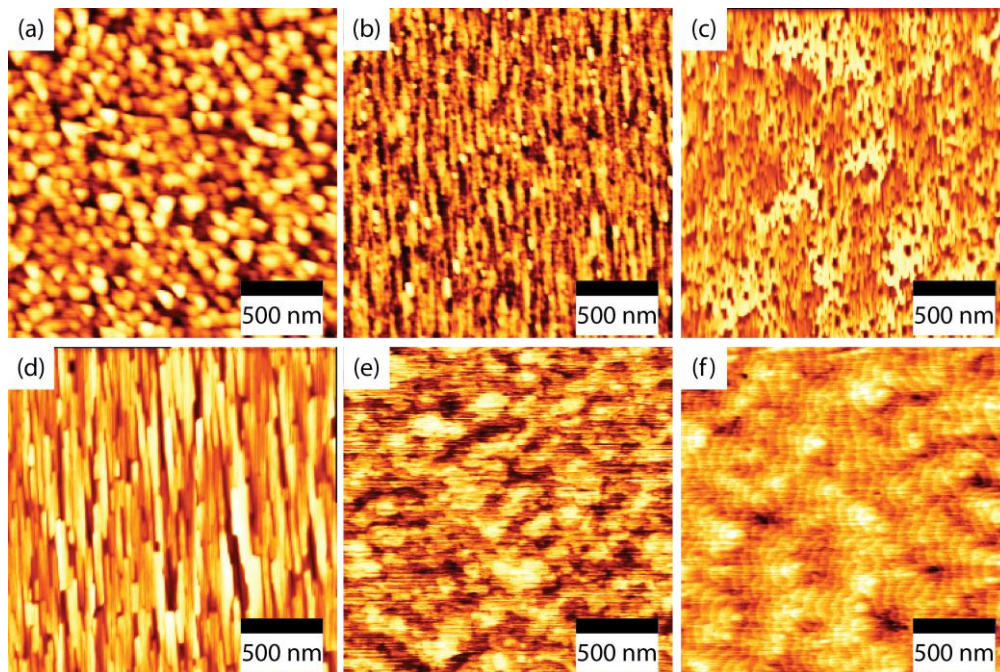


Figure 5: AFM topography of PZT 05/95 thin film on STO(110) substrate showing film growth improvements during optimization of PLD parameters.

Table 2: PLD deposition parameters for LSMO and PZT 05/95 thin films.

Material	Fluence ¹ [Jcm ⁻²]	Temp. ² [°C]	O ₂ ³ [mTorr]	Freq. ⁴ [Hz]	Distance ⁵ [cm]	Growth Rate [nm/100 Pulses]
LSMO	1.0	620	112	3	3.9	0.3
PZT 05/95	1.0	550	200	3	3.1	0.3

¹ Laser energy density calculated by dividing the laser energy by the laser spot size on the target.

² Temperature of the heated substrate holder, thus It can be slightly different from the actual substrate temperature depending on how it is measured.

³ Background oxygen pressure.

⁴ Laser pulse rate (frequency)

⁵ Substrate-target distance.

Structural Characterization

Figure 6 shows (110) peaks from 2theta-Omega XRD scan profiles of PZT 05/95 of different thicknesses (10, 60 and 107 nm) which were grown on STO(110) substrate with 10 nm LSMO bottom electrode. The only family of (110) peaks were detected in full range scan, indicating that the films were

single crystalline with (110) orientation. Low film roughness resulted in the manifestation of thickness fringes around the XRD peaks due to interference of X-rays reflected from the top and bottom interfaces of the thin film (Dorset, 1998). The periodicity of thickness fringes increases with film thicknesses (Figure 6 (a)-(b)), which eventually smoothen out in much thicker films (Figure 6 (c)).

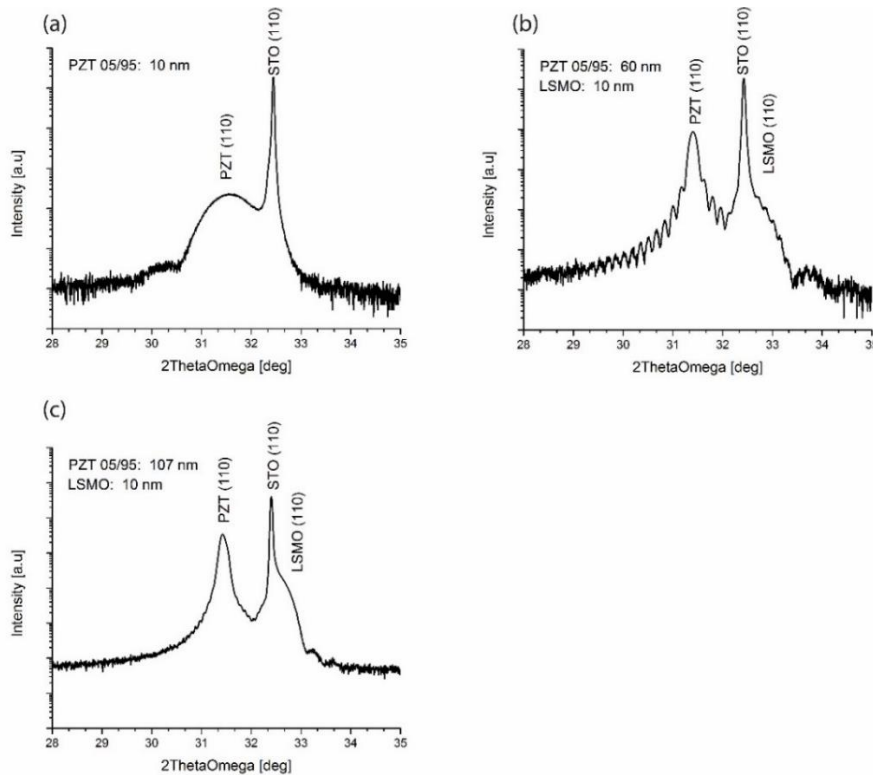


Figure 6: XRD 2theta-Omega images of PZT 05/95 thin films with different thicknesses with 10 nm LSMO on STO(110) substrate. (a) 10 nm PZT 05/95 thin film on ST(110), (b) 60 nm, and (c) 107 nm PZT 05/95 thin films.

Electrical Characterization

Electrical measurements were conducted by using a Piezoresponse force microscope (PFM) to study the polarization state of the as-grown films. The measurements were made by scanning $6\ \mu\text{m} \times 6\ \mu\text{m}$ regions of the film surface with conductive AFM tips at a scanning rate of 0.5 Hz and 256 lines as shown in Figure 7. The vertical PFM phase (Figure 7 (a)) shows that the as-grown films are single domain owing to the fact that there are no visible regions with domain walls or domains with different orientations.

To establish the actual orientation of the polarization vector, a positive 5 V d.c. voltage was applied on an AFM tip and used to pole part of the previously scanned film surface region. As shown in Figure 7, the switched region is in black contrast, indicating a 180° phase switching relative to the as-grown region. Since the switching was made possible by applying a positive voltage on the top film surface, it suggests that spontaneous polarization of as-grown films is pointing away from the substrate, also referred to as the c/c domain pattern as schematically shown in Table 8.

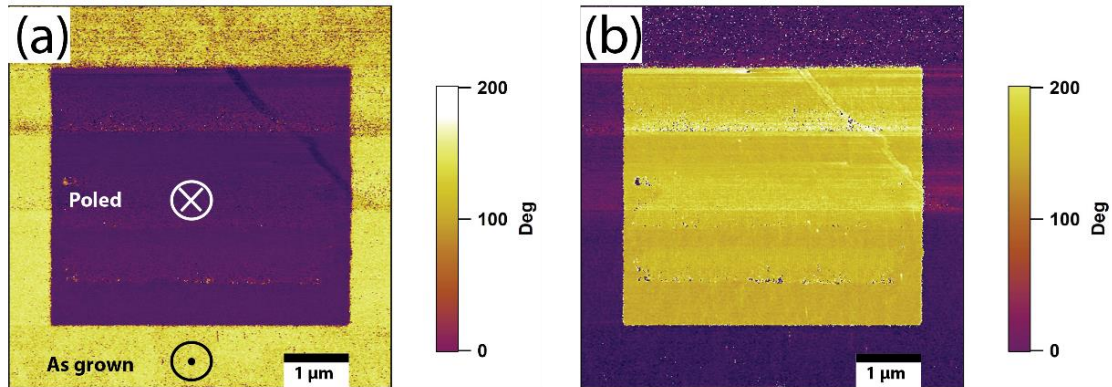


Figure 7: Vertical (a) and lateral (b) PFM phases of a 50 nm (110) PZT 05/95 film grown on STO(110) with 10 nm LSMO. PFM images indicate upwards as-grown monodomain structure and the downwards-poled central area which was switched by applying 5 V on the AFM tip.

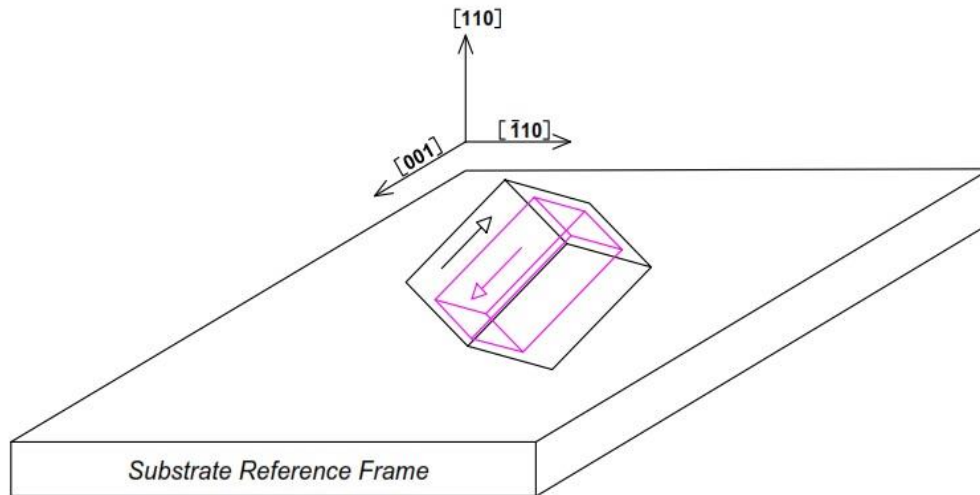


Figure 8: Schematic of c/c - domain pattern of tetragonal PZT in a (110) oriented substrate frame of reference.

CONCLUSIONS

Optimum PLD parameters for growing (110) oriented single-crystalline PZT 05/95 thin film on STO(110) substrate have been successfully achieved. It has been shown that double substrate termination hinders the step flow growth mode of the SRO bottom electrode regardless of substrate treatment. Despite inferior electrical conductivity properties, a thin layer of LSM bottom electrode was successfully deposited with step-flow growth mode on the substrate. This eventually enabled

the PZT film to grow with step flow growth mode on the electrode layer. Therefore, it can be concluded that the combination of optimized PLD conditions, low misfit strain as well as the quality of the bottom electrode has enabled the successful growth of (110) oriented PZT thin films. These findings are an important contribution to the processing techniques of complex oxide films. Furthermore, it was found that the work function difference between the bottom electrode and the PZT film dictates the preferential orientation of the film.

REFERENCES

- Ambika D., Kumar V., Imai H. and Kanno I. (2010). Sol-gel Deposition and Piezoelectric Properties of {110}-Oriented Pb (Zr_{0.52}Ti_{0.48})O₃ Thin Films. *Applied Physics Letters*, **96**(3): 031909. <https://doi.org/10.1063/1.3293446>
- Ambika D., Kumar V., Tomioka K. and Kanno I. (2012). Deposition of PZT Thin Films with (001), (110), and (111) Crystallographic Orientations and their Transverse Piezoelectric Characteristics. *Advanced Materials Letters*, **3**(2): 102-106. <http://dx.doi.org/10.5185/amlett.2011.7281>
- Antoni F. and Stock F. (2021). Laser Engineering of Carbon Materials for Optoelectronic Applications. Laser Annealing Processes in Semiconductor Technology. Elsevier.
- Bachelet R., Sánchez F., Santiso J., Munuera C., Ocal C. and Fontcuberta J. (2009). Self-assembly of SrTiO₃ (001) Chemical-terminations: A route for Oxide-Nanostructure Fabrication by Selective Growth. *Chemistry of Materials*, **21**(12): 2494-2498. <https://pubs.acs.org/doi/abs/10.1021/cm900540z>
- Baek S.-H., Choi S., Kim T. L. and Jang H. W. (2017). Domain Engineering in BiFeO₃ thin films. *Current Applied Physics*, **17**(5): 688-703. <https://doi.org/10.1016/j.cap.2017.02.016>
- Biswas A., Rossen P. B., Yang C. H., Siemons W., Jung M. H., Yang I. K., Ramesh R. and Jeong Y. H. (2011). Universal Ti-rich Termination of Atomically Flat SrTiO₃ (001),(110), and (111) Surfaces. *Applied Physics Letters*, **98**(5): 051904-051904. <https://doi.org/10.1063/1.3549860>
- Boschker H., Kautz J., Houwman E. P., Koster G., Blank D. H. and Rijnders G. (2010). Magnetic Anisotropy and Magnetization Reversal of La_{0.67}Sr_{0.33}MnO₃ Thin Films on SrTiO₃ (110). *Journal of Applied Physics*, **108**(10): 103906. <https://doi.org/10.1063/1.3506407>
- Chrisey D. B. and Hubler G. K. (2003). Pulsed Laser Deposition of Thin Films, 3rd ed., 1: 648, Wiley-VCH, New Jersey.
- Chu Y. H., Zhan Q., Martin L. W., Cruz M. P., Yang P. L., Pabst G. W., Zavaliche F., Yang S. Y., Zhang J. X. and Chen L. Q. (2006). Nanoscale Domain Control in Multiferroic BiFeO₃ Thin Films. *Advanced Materials*, **18**(17): 2307-2311. <https://doi.org/10.1002/adma.200601098>
- Damjanovic D. (1998). Ferroelectric, Dielectric and Piezoelectric Properties of Ferroelectric Thin Films and Ceramics. *Reports on Progress in Physics*, **61**(9): 1267-1267. <http://dx.doi.org/10.1088/0034-4885/61/9/002>
- Dorset D. (1998). X-Ray Diffraction: A Practical Approach, **4**: 513-515.
- Kim K.-C., Kim S. K., Kim J.-S. and Baek S.-H. (2020). Domain Engineering of Epitaxial (001) Bi₂Te₃ Thin Films by Miscut GaAs Substrate. *Acta Materialia*, **197**: 309-315. <https://doi.org/10.1016/j.actamat.2020.07.051>
- Koster G., Klein L., Siemons W., Rijnders G., Dodge J. S., Eom C.-B., Blank D. H. A. and Beasley M. R. (2012). Structure, Physical Properties, and Applications of SrRuO₃ Thin Films. *Reviews of Modern Physics*, **84**(1): 253-253. <https://doi.org/10.1103/RevModPhys.84.253>
- Ma J., Liu X., Lin T., Gao G., Zhang J., Wu W., Li X. and Shi J. (2009). Interface Ferromagnetism in (110)-oriented La_{0.7}Sr_{0.3}MnO₃/SrTiO₃ ultrathin superlattices. *Physical Review B*, **79**(17): 174424. <http://dx.doi.org/10.1103/PhysRevB.79.174424>
- Majumdar S., Kooser K., Elovaara T., Huhtinen H., Granroth S. and Paturi P. (2013). Analysis of electronic structure and its effect on magnetic properties in (001) and (110) oriented La_{0.7}Sr_{0.3}MnO₃ thin films. *Journal of Physics: Condensed Matter*, **25**(37): 376003. <http://dx.doi.org/10.1088/0953-8984/25/37/376003>
- Mtebwa M., Tagantsev A. K. and Setter N. (2014). Effect of elastic compliances and higher order Landau coefficients on the phase diagram of single domain epitaxial Pb (Zr, Ti)O₃ (PZT) thin films. *AIP Advances*, **4**(12): 127150-127150. <http://dx.doi.org/10.1063/1.4905265>
- Mtebwa M. H. and Setter N. (2022). Pulsed Lased Deposition of Single-Crystalline (001) Oriented Pb(Zr_{0.5}Ti_{0.5})O₃ Thin Film on PrScO₃ Substrate. *Tanzania Journal of Science*, **48**(3): 528-536. <https://dx.doi.org/10.4314/tjs.v48i3.1>
- Schwarzkopf J., Braun D., Hanke M., Uecker R. and Schmidbauer M. (2017). Strain Engineering of Ferroelectric Domains in K_xNa_{1-x}NbO₃ epitaxial layers. *Frontiers in Materials*, **4**: 26. <https://doi.org/10.1088/1361-6528/aa715a>
- Sun F., Chen D., Gao X. and Liu J.-M. (2021). Emergent Strain Engineering of Multiferroic

Optimization of Pulsed Laser Deposition Parameters for Single-Crystalline (011) Oriented Tetragonal Pzt Thin

- BiFeO₃ thin films. *Journal of Materiomics*, **7**(2): 281-294. <https://doi.org/10.1016/j.jmat.2020.08.005>
- Tagantsev A. K., Cross L. E. and Fousek J. (2010). Domains in Ferroic Crystals and Thin Films, Springer, New York.
- Vafaee M., Baghaie Yazdi M., Radetinac A., Cherkashinin G., Komissinskiy P. and Alff L. (2013). Strain Engineering in Epitaxial La_{1-x} Sr_{1+x} MnO₄ thin films. *Journal of Applied Physics*, **113**(5): 053906. <http://dx.doi.org/10.1063/1.4790654>
- Vu H. T., Nguyen M. D., Houwman E., Boota M., Dekkers M., Vu H. N. and Rijnders G. (2015). Ferroelectric and Piezoelectric Responses of (110) and (001)-Oriented Epitaxial Pb(Zr_{0.52} Ti_{0.48})O₃ thin films on all-oxide layers buffered silicon. *Materials Research Bulletin*, **72**: 160-167. <https://doi.org/10.1016/j.materresbull.2015.07.043>
- Wada S., Kakemoto H. and Tsurumi T. (2004). Enhanced Piezoelectric Properties of Piezoelectric Single Crystals by Domain Engineering. *Materials Transactions*, **45**(2): 178-187. <http://dx.doi.org/10.1557/PROC-785-D1.2>
- Wada S., Muraishi T., Yokoh K., Yako K., Kamemoto H. and Tsurumi T. (2007). Domain Wall Engineering in Lead-Free Piezoelectric Crystals. *Ferroelectrics*, **355**(1): 37-49. <https://doi.org/10.1080/00150190701515881>
- Wada S., Park S.-E., Cross L. E. and Shrout T. R. (1999). Engineered Domain Configuration in Rhombohedral PZN-PT Single Crystals and their Ferroelectric Related Properties. *Ferroelectrics*, **221**(1): 147-155. <https://doi.org/10.1080/00150199908016449>
- Wada S., Park S. E., Cross L. E. and Shrout T. R. (1998). Domain Configuration and Ferroelectric related Properties of Relaxor based Single Crystals. *Journal of the Korean Physical Society*, **32**: 1290-1293.
- Wada S. and Tsurumi T. (2004). Enhanced Piezoelectricity of Barium Titanate Single Crystals with Engineered Domain Configuration. *British ceramic transactions*, **103**(2): 93-96.
- Willmott P. R. and Huber J. R. (2000). Pulsed Laser Vaporization and Deposition. *Reviews of Modern Physics*, **72**(1): 315-315. <https://doi.org/10.1103/RevModPhys.72.315>